Properties of $(CH_3)_2NH_2H_2PO_4$ crystal near the ferroelectric phase transition

2008 J. Phys.: Condens. Matter 20 215222

(http://iopscience.iop.org/0953-8984/20/21/215222)

J. Phys.: Condens. Matter **20** (2008) 215222 (7pp) doi:10.1088/0953-8984/20/21/215222

Properties of $(CH_3)_2NH_2H_2PO_4$ crystal near the ferroelectric phase transition

A Nowak, S Dacko, J Przesławski and Z Czapla

Institute of Experimental Physics, Wrocław University, pl. M. Borna 9, 50-204 Wrocław, Poland

E-mail: a.hek@ifd.uni.wroc.pl (A Nowak)

Received 10 December 2007, in final form 7 March 2008
Published 24 April 2008
Online at stacks.iop.org/JPhysCM/20/215222

Abstract

The results of dielectric, thermal (AC calorimetry) and dilatometric measurements on DMAP crystal in the ferroelectric phase transition region are presented. The experimental data are discussed in the framework of the Landau theory, and expansion coefficients of the Landau potential A_0, B, C are estimated. A temperature dependence of the effective nonlinearity coefficient B has been revealed. The pressure coefficient dT_c/dp was obtained. The phase transition can be classified as a continuous one and rather far from the tricritical point. The specific heat data show a λ-type anomaly and the value of the excess entropy is smaller than in typical order–disorder phase transitions.

1. Introduction

One of the most important groups of crystals with hydrogen bonds is the group with the general chemical formula AH_2BO_4, where A = K, Rb, Cs, NH_4, $(CH_3)_2NH_2$ and B = P, As. There are two subfamilies in the AH_2BO_4 group: tetragonal (representative: KH_2PO_4) and monoclinic (representative: CsH_2PO_4). Hatori *et al* [1] reported that $(CH_3)_2NH_2H_2PO_4$ (abbreviated as DMAP), which belongs to the second subfamily, undergoes a ferroelectric phase transition at $T_c = 259.15$ K from the monoclinic space group $P2_1/n$ at room temperature to the Pn space group in the ferroelectric phase. The spontaneous polarization vector lies in the ac plane and is inclined from the c axis towards the a axis by an angle of 17°. According to dielectric relaxation studies [2] the mechanism of the phase transition is of the order–disorder type. X-ray structural analysis shows that there are two kinds of hydrogen bond chains in the structure [1, 3]. It should be mentioned that in a system of axes given by Pietraszko *et al* [3] the a axis is interchanged with the c axis in relation to the system reported in [1]. The hydrogens of weaker hydrogen bonds linking the PO_4 groups along the b axis are ordered at room temperature (the paraelectric phase). Those along the c axis [1], linking the PO_4 tetrahedra into zigzag chains seem to be disordered above T_c. So the phase transition is connected to an ordering of the hydrogen bonds in the phosphate chains parallel to the c axis. In both phases $(CH_3)_2NH_2$ cations are ordered and the reorientation of cation groups cannot be regarded as the mechanism of the transition. The significant isotope effect on the phase transition temperature arising from deuteration suggests that the hydrogens do indeed play a main role in the transition.

The aim of our studies is obtaining detailed characteristics of the paraelectric–ferroelectric phase transition in DMAP crystal by carrying out complex studies of dielectric, specific heat and dilatometric properties.

2. Experiment

The single crystals of $(CH_3)_2NH_2H_2PO_4$ were obtained by a slow evaporation method, from water solutions containing stoichiometric quantities of 40% water solutions of $(CH_3)_2NH$ and H_3PO_4 at 303 K. The c^* plates, of thickness 1.0 mm and area about 16 mm^2, in the ferroelectric direction, were cut out from the single crystal. Silver paste films were used as electrodes. The capacitance of the samples was measured using a precision LCR-meter HP 4284A at the frequency of 10 kHz and amplitude of 1×10^{-2} V mm^{-1}. The temperature dependences of the electric permittivity were measured in a cooling run with the rate 0.5 K min^{-1} under dc electric field ranging from 0 to 1000 kV m^{-1}. In the paraelectric phase in the temperature range $T_c + 13$ K an electric field of amplitude 225 kV m^{-1} and frequency 2×10^{-3} Hz was applied to the sample at constant temperature to measure the field dependence of the permittivity. During this experiment the temperature was stabilized with an accuracy

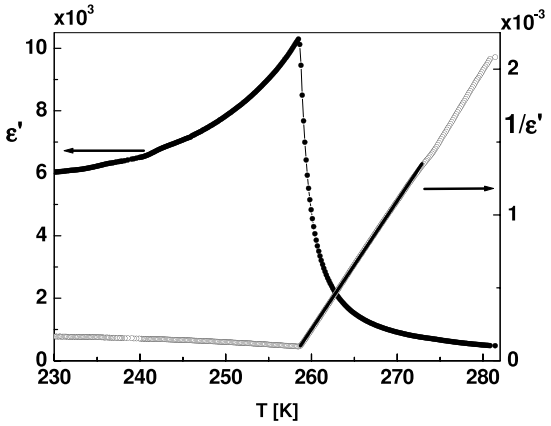

Figure 1. Temperature dependence of the electric permittivity and its reciprocal for DMAP measured along the ferroelectric c^* direction.

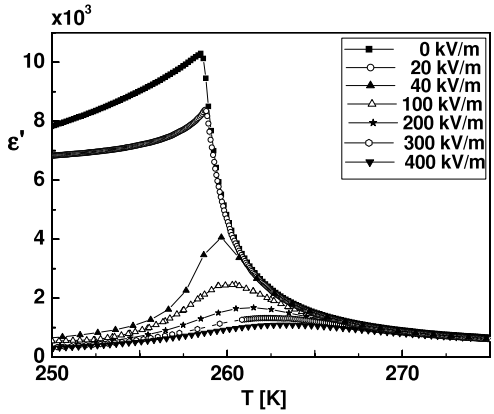

Figure 2. Temperature dependence of the electric permittivity at various dc electric fields.

not worse than 5×10^{-3}. The temperature dependence of the spontaneous polarization was obtained from measurements of the pyroelectric current. The thermal expansion was investigated using a quartz precision capacitance dilatometer. The capacitance was measured using an HP 4284A LCR-meter at frequency 1.2 kHz. For dilatometric measurements, the specimens were cut out along three crystallographic directions, with the dimensions 2–4 mm.

The temperature dependence of the specific heat was measured using an AC calorimeter Sinku-Riko system, model ACC-1M/L. The specific heat measurements were performed while heating and cooling with a constant rate of 0.1 K min^{-1}. The temperature of the heat bath was measured using a platinum resistance thermometer with a resolution of 0.01 K. The ac temperature amplitude at a frequency of 1 Hz was measured using a JIS 'E' type thermocouple with a resolution of 0.0025 K.

3. Results and discussion

3.1. Temperature dependence of the permittivity

The electric permittivity measured in the c^* direction is presented in figure 1.

The maximum value of the electric permittivity is about 11×10^3 and it is comparable to that presented in the paper [1]. For the paraelectric phase the Curie–Weiss law

$$\varepsilon' = \frac{C_{\mathrm{cw}}}{T - T_{\mathrm{c}}} \tag{1}$$

is well fulfilled in the measuring temperature range (see figure 1) with $C_{\mathrm{cw}} = (11.40 \pm 0.01) \times 10^3$ K, and $T_{\mathrm{c}} = 258.50 \pm 0.05$ K.

In figure 2 the temperature variations of the electric permittivity measured under dc bias fields of various intensities are shown. The maximum of the electric permittivity decreases significantly with increase of the applied electric field strength. In addition the position of the maximum shifts to higher temperatures. Such behavior of the crystal in electric dc fields is characteristic of ferroelectric continuous phase transitions.

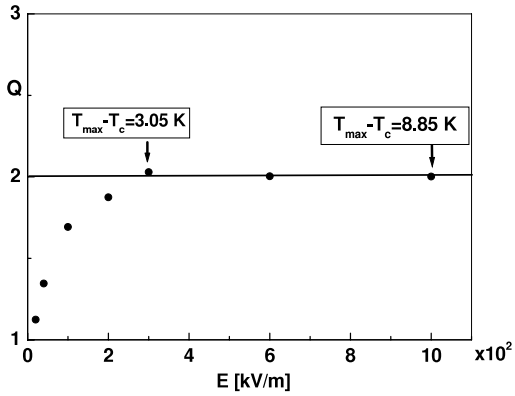

Figure 3. Field dependence of the coefficient Q defined as $Q = \varepsilon'(T_{\max}, E = 0)/\varepsilon(T_{\max}, E)$.

In order to describe experimental data the classical dielectric state equation, derived from Landau theory, was used:

$$E = A_0(T - T_{\mathrm{c}})D + BD^3 + CD^5. \tag{2}$$

First, we investigate the ratio [4, 5]

$$Q = \frac{\varepsilon'(T_{\max}, E = 0)}{\varepsilon(T_{\max}, E)}, \tag{3}$$

where $T_{\max}$ denotes the temperature of the maximum value of the electric permittivity $\varepsilon'(T_{\max}, E)$ for a given value of the electric field E. In figure 3 the variations of the Q values obtained for DMAP crystal are presented. As can be seen, the coefficient changes considerably for low electric fields, in the temperature region close to T_{c}, but for higher values of the electric field it is equal to 2, the value expected within the framework of Landau theory [4].

The value of the coefficient $A_0 = (9.80 \pm 0.01) \times 10^6$ m F^{-1} K^{-1} was directly obtained from the relation $A_0 = (\varepsilon_0 C_{\mathrm{cw}})^{-1}$. The nonlinear coefficient B was calculated from the field dependence of the maximum electric permittivity ($\varepsilon = \varepsilon_0 \varepsilon'$) [6]:

$$(\varepsilon_{\max})^{-1} = \frac{3}{2^{1/3}} B^{1/3} E^{2/3}, \tag{4}$$

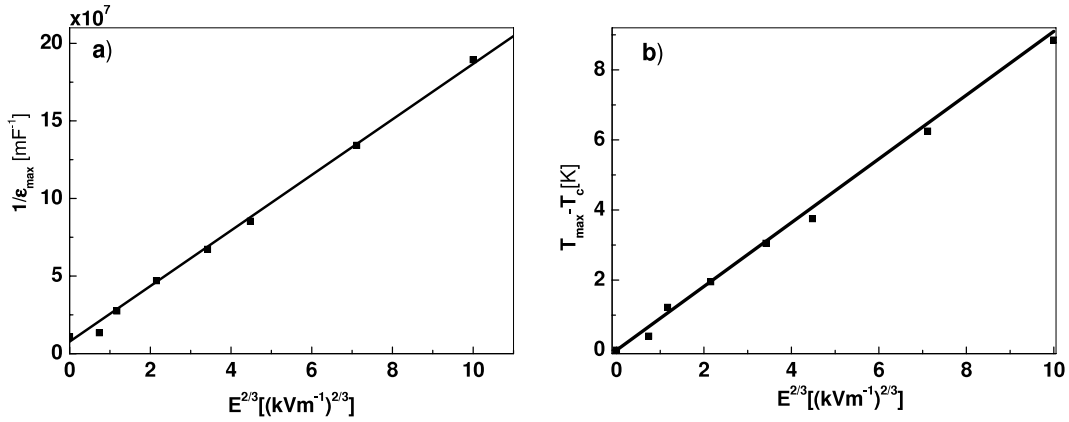

Figure 4. (a) Maximum of the electric permittivity $(\varepsilon_{\max})^{-1}$ versus $E^{2/3}$. (b) Temperature of the maximum permittivity $T_{\max}$ versus dc electric field E.

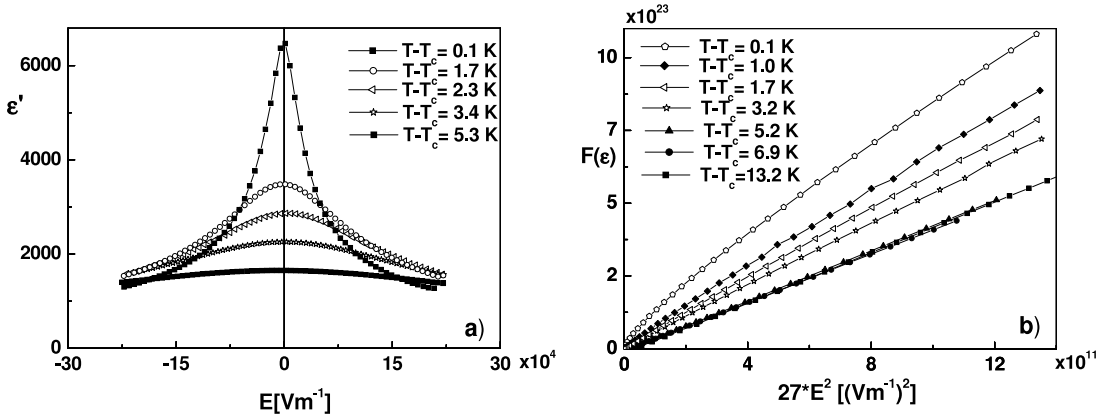

Figure 5. (a) Field dependence of the electric permittivity at some temperatures in the paraelectric phase. (b) Plot of the function $F(\varepsilon)$ (see equation (6)) versus $27\,E^2$, for $T > T_c$.

derived from the equation (2), using the first two terms only. The linear dependence of $\varepsilon_{\max}^{-1}$ as a function of $E^{2/3}$, presented in figure 4(a), shows that equation (4) is well fulfilled in the electric field range considered. The nonlinearity coefficient B is equal to $(4.10 \pm 0.10) \times 10^{11}$ V m^5 C^{-3}. As can be seen in figure 2(a), the maximum of the permittivity shifts to higher temperatures, and the temperature $T_{\max}$ can be expressed according to the formula [6, 7]

$$T_{\max} = T_c + \frac{3B^{1/3}}{2^{4/3}A_0}(E)^{2/3}. \qquad (5)$$

The experimental data are presented in figure 4(b). The solid line in figure 4(b) was calculated using equation (5) for the A_0 and B presented above. It is worth noticing that the maximum of the permittivity shifts to higher temperatures significantly, by about 8 K under the field of 900 kV m^{-1}.

3.2. Field dependence of the permittivity at constant temperatures

The further studies were focused on the dc electric field dependence of the electric permittivity at constant temperatures in the paraelectric phase. The measurements were performed in the range of temperature $T_c + 13.5$ K. In figure 5(a), as examples, the field dependences of the electric permittivity at several temperatures are presented. In order to describe experimental data we started from the thermodynamic theory. The dielectric state equation (2) (limited to the D^3 term) can be changed into another equivalent form [8]:

$$F(\varepsilon') = \left(\frac{1}{\varepsilon'}\right)^3 + \frac{3}{\varepsilon(0)}\left(\frac{1}{\varepsilon'}\right)^2 - 4\left(\frac{1}{\varepsilon(0)}\right)^3 = 27BE^2, \quad (6)$$

putting together the external electric field E, the electric permittivity ε_0 measured at zero electric field and the non-zero-field permittivity ε. Then, the temperature and the electric displacement D are eliminated from equation (2).

Results for a few chosen temperatures are illustrated in figure 5(b). As is shown, the different isothermal data are not lying on one straight line when the temperature is close to T_c. However, for the temperatures greater than $T_c + 3$ K, isotherms are on the same straight line.

The values of the nonlinearity coefficient B, which were obtained from the slope of lines presented, in figure 5(b), are presented in figure 6. One can see that, for temperature greater then $T_c + 3$ K, B is temperature independent and equal to

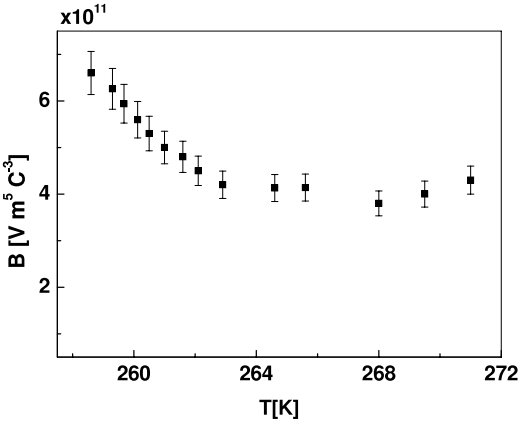

Figure 6. Temperature variation of the effective coefficient B in the paraelectric phase.

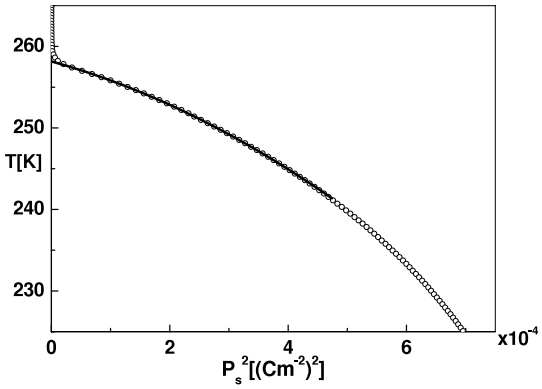

Figure 7. Temperature T versus P_s^2; circles denote experimental data, while the solid line was calculated according to equation (7).

$(4.00\pm0.10)\times10^{11}$ V m^5 C^{-3}. This value is in good agreement with the one calculated from the dependence (4).

3.3. Spontaneous polarization

The spontaneous polarization was obtained from the pyroelectric current measurements. To have a monodomain state we applied an electric field with the intensity of 20 kV m^{-1} to the sample. The spontaneous polarization is equal to 3.2×10^{-2} C m^{-2} at the temperature 200 K and this value is the same as that reported in the previous paper [1]. However, the results obtained gave a very precise dependence $P_s(T)$ near T_c.

To describe the experimental data the following expression was used:

$$T = T_c - \beta P_s^2 - \gamma P_s^4, \tag{7}$$

where $\gamma = C/A_0$, $\beta = B/A_0$. This relation was calculated from equation (2) (with the term D^5).

In figure 7, $T(P_s^2)$ is presented; the solid line represents the best fit of equation (7) to experimental data with $T_c = 258.75 \pm 0.05$ K, $B = (1.10 \pm 0.08)\times10^{11}$ V m^5 C^{-3}, $C = (3.30\pm0.10)\times10^{14}$ V m^9 C^{-5}.

The parameter $V = B/(A_0C)^{1/2}$ [9] can be used to characterize the order of the phase transition [10]. The physical meaning of this parameter gives a sign for V (for the second-order phase transition $V > 0$, but for the first-order one $V < 0$). The square of V can indicate, in kelvins, the proximity of the transition to the tricritical one. The value of this parameter is equal to 1.74 K$^{1/2}$ and 3.20 K$^{1/2}$ for TGS [8, 11] and TAAP [12] crystals, respectively. These crystals exhibit a second-order phase transition. For the TGSe crystal, in which the transition is close to the tricritical one [10], $V = 0.44$ K$^{1/2}$. For the DMAP crystal the parameter V is equal to 3.10 K$^{1/2}$ which evidences the continuous character of the transition.

It is worth noticing that the critical exponent β, which was determined as the slope of $\log(P_s)$ versus $\log(T_c - T)$, is equal to 0.41 ± 0.02. This value is comparable to the one reported in [13, 14], and is far from the value of 0.25 predicted for the tricritical case.

3.4. Specific heat measurements

The temperature dependence of the molar heat capacity of DMAP crystals is shown in figure 8(a). To estimate the amount of excess heat capacity due to the ferroelectric phase transition, the contribution of the normal heat capacity must be subtracted from the measured molar heat capacity. For this crystal the background (lattice) heat capacity was approximated by a third-order polynomial. The excess of the molar specific heat capacity ΔC_p is presented in figure 8(b). The anomaly appears at a temperature of about 260.00 ± 0.05 K and it is connected to the phase transition. One can see that the measured ΔC_p has a shape typical for a continuous phase transition and at $T = T_c$, ΔC_p is equal to 7.33 ± 0.01 J K^{-1} mol^{-1}. In the next step the specific heat critical index α was obtained (see figure 9) from the slope of $\log(\Delta C_p)$ versus $\log(T_c - T)$. The value of α is equal to -0.0070 ± 0.0003 so it is close to zero. This value of the critical index α is typical for a mean field model of a phase transition [15]. The Landau theory gives a simple relation between the excess entropy and the order parameter:

$$\Delta S(T) = -\tfrac{1}{2}A_0 P_s^2. \tag{8}$$

Further information about the nature of the phase transition can be obtained from the excess entropy (ΔS). The most direct way to determine ΔS is from measurements of the excess specific heat as a function of temperature:

$$\Delta S(T) = \int_{T_0}^{T} \frac{\Delta C_p}{T}\mathrm{d}T. \tag{9}$$

The transition entropy calculated from the above equation is equal to $\Delta S = 0.50 \pm 0.04$ J K^{-1} mol^{-1} and it is smaller than that calculated from equation (8), where $\Delta S = 0.65 \pm 0.05$ J K^{-1} mol^{-1}. This value of the excess entropy is similar to the ΔS value found for isomorphous $(CH_3)_2NH_2H_2AsO_4$ crystal [16] ($\Delta S = 0.95$ J(K mol)$^{-1}$ and $\Delta C_p = 7.0$ J(K mol)$^{-1}$), and to the excess of entropy ΔS determined for other representative crystals of the AH_2BO_4 group belonging to the monoclinic system, e.g. CsH_2PO_4 [17] ($\Delta S = 1.05$ J(K mol)$^{-1}$). The order–disorder model in the mean field theory gives the transition entropy of $R\ln 2 = 5.76$ J(K mol)$^{-1}$, which is several times the experimental

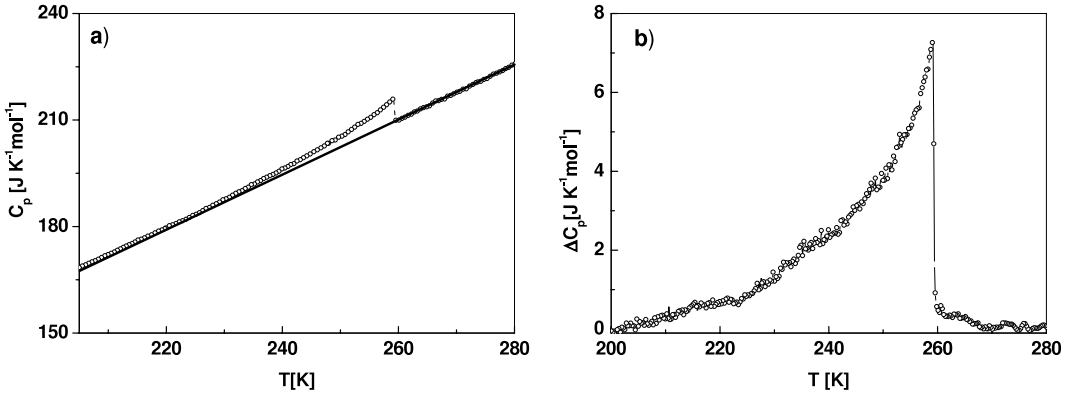

Figure 8. (a) Temperature dependence of the specific heat for the DMAP crystal measured using the AC calorimetry technique (brown line: crystal background). (b) The specific heat excess (δC_p) as a function of temperature for DMAP crystal (ferroelectric phase).

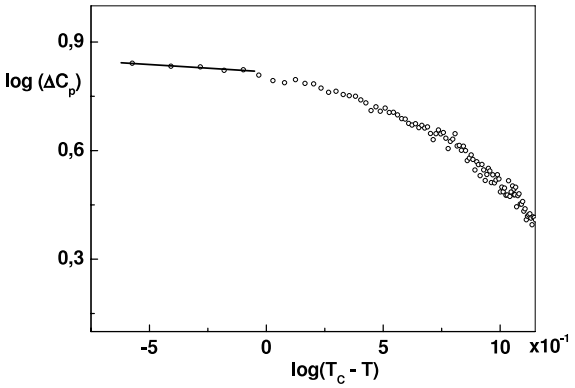

Figure 9. Temperature dependence of the specific heat (log–log plot).

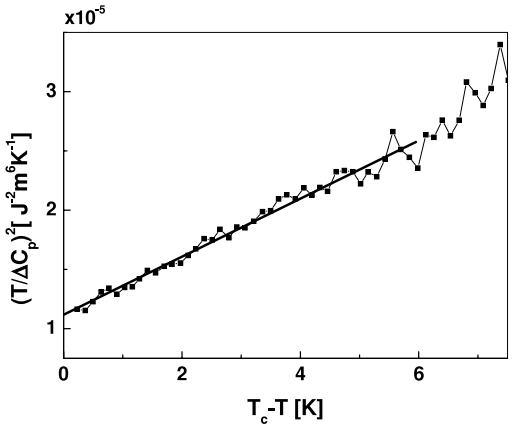

Figure 10. Dependence of $(T/\Delta C_p)^2$ on T (squares: experimental data; solid line: fitting line according to equation (10)).

value. It seems inevitable that we must take a tunneling mechanism [18] into account, which can greatly reduce this discrepancy with the experiment.

Further, taking into account equation (8) and the relation $\Delta C_p = T\ \partial \Delta S/\partial T$ one obtains

$$\left(\frac{T}{\Delta C_p}\right)^2 = \frac{4B^2}{A_0^4} + \frac{16C}{A_0^3}\,(T_c - T)\,. \tag{10}$$

Equation (10) enables us to determine the magnitude of the coefficients B and C. As was mentioned above, for the DMAP crystal the parameter A_0 is equal to $9.80 \pm 0.01 \times 10^6$ m F^{-1} K^{-1}. Figure 10 shows the temperature dependence of $(T/\Delta C_p)^2$. One can see that equation (10) is fulfilled at least 5.5 K below the temperature of the phase transition. The coefficients B and C are equal to $(1.59\pm0.10)\times10^{11}$ V m^5 C^{-3} and $(1.43 \pm 0.11) \times 10^{14}$ V m^9 C^{-5}, respectively.

4. Dilatometric measurements

Measurements of the thermal linear expansion along the a, b and c axes were performed. The temperature dependences of the linear expansions are shown in figures 11 and 12.

When the crystal is cooled, it contracts in the three crystallographic directions. A clear anomaly of the relative elongation $(\Delta l/l_0)$ of the samples was observed along the a crystallographic direction at the temperature of about 260.00 ± 0.05 K. This anomaly is characteristic for a continuous phase transition. Similar behaviors were observed during x-ray measurements [3], though they were not precise in the vicinity of T_c.

It is well known that the linear thermal expansion has the form

$$\alpha_i = \frac{1}{l_0}\left(\frac{\partial l}{\partial T}\right)_{p,E}. \tag{11}$$

We estimated the linear thermal expansion coefficient according to equation (11). In figures 11 and 12 it can be seen that only α_a changes its value at the temperature of the phase transition; the α_b and α_c changes are negligible.

The volume thermal expansion coefficient can be calculated as

$$\alpha_v = \alpha_a + \alpha_b + \alpha_c. \tag{12}$$

Taking into account the anomaly at T_c, which was observed along the a axis, the jump in the volume thermal expansion coefficient will be equal to the jump in the linear thermal coefficient α_a. $\Delta\alpha_v = \Delta\alpha_a = -2.0 \pm 0.2 \times 10^{-5}$ K^{-1}.

The anomaly in α_v corresponds to the anomaly in the specific heat near the temperature of the phase transition. The

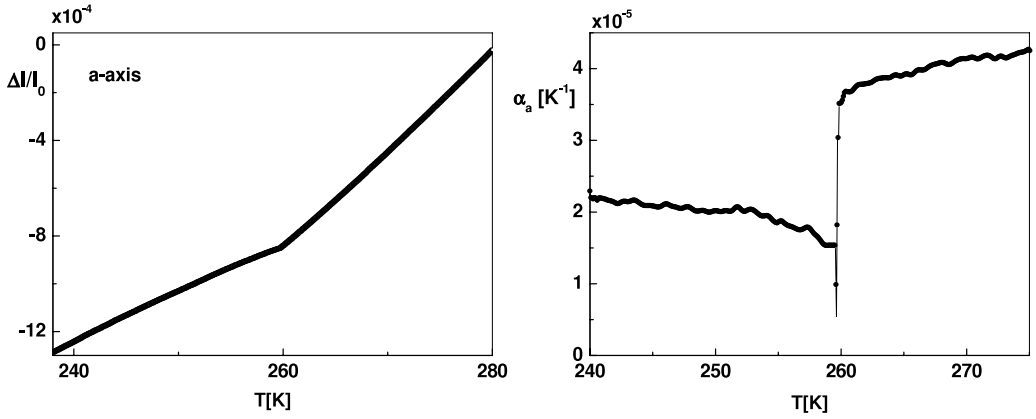

Figure 11. Temperature dependence of the linear thermal expansion $\Delta l/l_0$ and the linear expansivity α_a.

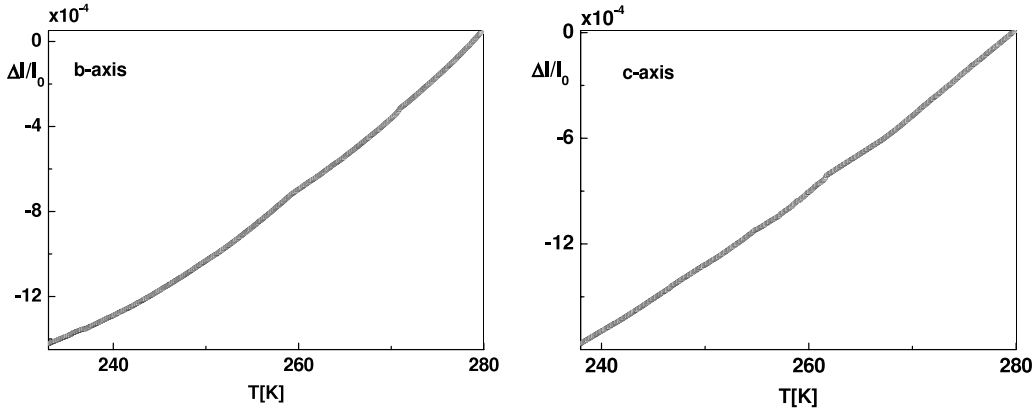

Figure 12. Temperature dependence of the linear thermal expansion $\Delta l/l_0$.

Ehrenfest equation connects α_v and ΔC_p:

$$\frac{\mathrm{d}T_\mathrm{c}}{\mathrm{d}p} = T_\mathrm{c}\frac{V_\mathrm{m}\Delta\alpha_v}{\Delta C_p}, \tag{13}$$

where p is the hydrostatic pressure, V_m is the molar volume which is equal to 93.46×10^{-6} m^3 mol^{-1}, ΔC_p is the jump of the heat capacity at T_c which is equal to 7.33 ± 0.01 J K^{-1} mol^{-1}, and $\Delta\alpha_v$ is the change in the volume thermal expansion coefficient at T_c. Using the above mentioned data we calculated $\mathrm{d}T_\mathrm{c}/\mathrm{d}p = -6.6 \pm 0.6 \times 10^{-8}$ K m^3 J^{-1}. This calculated value is in good agreement with experimental one obtained in [19] ($\mathrm{d}T_\mathrm{c}/\mathrm{d}p = -6.4 \times 10^{-8}$ K m^3 J^{-1}).

5. Summary

The results of our work can be summarized as follows:

- The experimental results obtained give the first quantitative description of the dielectric and thermal properties of the DMAP crystal in the framework of the Landau theory.
- The Landau expansion coefficients A_0, B and C were estimated using various methods. Values of the B and C coefficients are collected in the table below. It is worth noting that B and C coefficients obtained from P_s^2 and the ΔC_p data can be attributed to the ferroelectric phase. A higher value of the coefficient B was derived for the paraelectric phase (from the $\varepsilon_\mathrm{max}(E)$ and $F(\varepsilon)(27B^2)$ methods).

Method	$B \times 10^{11}$ V m^5 C^{-3}	$C \times 10^{14}$ V m^9 C^{-5}
$\varepsilon_\mathrm{max}(E)$	4.10 ± 0.10	—
$F(\varepsilon)(27B^2)$	4.00 ± 0.10	—
$T(P_\mathrm{s}^2)$	1.10 ± 0.08	3.30 ± 0.10
$(T/\Delta C)^2(T)$	1.59 ± 0.10	1.43 ± 0.11

- Results of dielectric and heat capacity measurements confirmed that the phase transition is a continuous one.
- Dilatometric measurements confirm the existence of a continuous phase transition at 260.00 ± 0.05 K, and a pressure coefficient (according to the Ehrenfest equation) equal to $\mathrm{d}T_\mathrm{c}/\mathrm{d}p = -6.6 \pm 0.6 \times 10^{-8}$ K m^3 J^{-1} was obtained.
- The ΔS value is comparable to the ones reported for the isomorphous arsenate analog crystal and for the main representative crystal of the group: CsH_2PO_4. The proton tunneling mechanism should be taken into account to explain the smaller values of the excess entropies measured for these crystals. However, the Landau theory relation between the excess entropy and the order

parameter described by equation (8) is fulfilled quite well, so the theory used was justified.

References

[1] Hatori J, Komukae M, Osaka T and Makita Y 1996 *J. Phys. Soc. Japan* **65** 1960
[2] Komukae M, Irieda T, Hatori J and Osaka T 1998 *Ferroelectrics* **219** 745
[3] Pietraszko A, Kucharczyk D and Pawłowski A 1999 *J. Mol. Struct.* **508** 139
[4] Westwański B and Fugiel B 1991 *Phys. Rev.* B **43** 3637
[5] Otolińska A and Westwański B 2000 *J. Phys.: Condens. Matter* **12** 1473
[6] Bornarel J and Schmidt V H 1981 *J. Phys. C: Solid State Phys.* **14** 2017
[7] Lines M E and Glass AM 1977 *Principles and Applications of Ferroelectrics and Related Materials* (Oxford: Clarendon)
[8] Cach R, Jaśkiewicz A and Lamber R 1982 *Acta Phys. Pol.* A **62** 249
[9] Gergs M K, Michel D, Schlemmbach H and Windsch W 1986 *J. Phys. D: Appl. Phys.* **19** 2431
[10] Cach R 1993 *Dielectric Non-Linear Properties of Some Real Ferroelectric Crystals* (Wrocław: Wrocław University Press)
[11] Ehses K H and Müser H E 1976 *Ferroelectrics* **12** 247
[12] Cach R and Czapla Z 1990 *Phys. Status Solidi* a **121** 299
[13] Czapla Z, Furtak J, Kosturek B, Hatori J and Osaka T 1999 *Ferroelectrics* **223** 51
[14] Przesławski J, Dacko S, Hatori J and Komukae M 2000 *Phys. Status Solidi* b **219** 395
[15] Strukov B A and Levanyuk A P 1998 *Ferroelectric Phenomena in Crystals* (Berlin: Springer)
[16] Hatori J, Tsuri K, Deguchi K, Komukae M and Osaka T 1998 *Ferroelectrics* **219** 115
[17] Kanda E, Yoshizawa M, Yamakami T and Fujimura T 1982 *J. Phys. C: Solid State Phys.* **15** 6823
[18] Kojyo N and Onodera Y 1988 *J. Phys. Soc. Japan* **57** 12 4391
Vaks V, Zein N and Strukov B 1975 *Phys. Status Solidi* a **30** 801
[19] Yamada T, Hatori J, Shikanai F, Komukae M and Osaka T 2000 *J. Phys. Soc. Japan* **69** 288